

Cosmological Acceleration and Gravitational Collapse

Pantelis S. Apostolopoulos[†], Nikolaos Brouzakis, Nikolaos Tetradiis and Eleftheria Tzavara

University of Athens, Department of Physics, Nuclear and Particle Physics Section,
Panepistimiopolis, Zografos 15771, Athens, Greece

Abstract. The acceleration parameter defined through the local volume expansion is negative for a pressureless, irrotational fluid with positive energy density. In the presence of inhomogeneities or anisotropies the volume expansion rate results from averaging over various directions. On the other hand, the nature of the expansion deduced through the observation of light from a certain source in the sky is specific to the direction to that source. If there are preferred directions in the underlying geometry one can define several expansion parameters. We provide such definitions for the case of the Tolman-Bondi metric. We then examine the effect of a localized inhomogeneity on the surrounding cosmological fluid. Our framework is similar in spirit to the model of spherical collapse. For an observer in the vicinity of a central overdensity, the perceived local evolution is consistent with acceleration along the radial direction, and deceleration perpendicularly to it. A negative mass leads to deceleration along the radial direction, and acceleration perpendicularly to it. If the observer is located at the center of an overdensity the null geodesics are radial. The form of the luminosity distance as a function of the redshift is consistent with acceleration for a certain range of redshifts.

[†] E-mail: vdfspap8@uib.es

1. Introduction

The cosmological expansion of our Universe seems to have accelerated in the recent past. This conclusion is supported by the form of the luminosity distance as a function of the redshift for distant supernovae [1, 2]. In the context of homogeneous cosmology, a recent accelerating phase is also in agreement with the observed perturbations in the cosmic microwave background [3]. The mechanism that triggered the acceleration has not been identified conclusively. The simplest explanation is that the cosmological constant is non-zero. However, the absence of acceleration at redshifts $z \gtrsim 1$ implies that the required value of the cosmological constant is approximately 120 orders of magnitude smaller than its natural value in terms of the Planck scale.

One intriguing fact is that the accelerating phase coincides with the period in which inhomogeneities in the matter distribution at length scales $\lesssim 10$ Mpc become significant, so that the Universe cannot be approximated as homogeneous any more at these scales. A link between inhomogeneities and cosmological acceleration has been pursued in various studies. There have been arguments, based on perturbative estimates, that the backreaction of superhorizon inhomogeneities on the cosmological expansion is significant and could cause the acceleration [4]. However, the validity of this effect is questionable [5].

We are interested in the importance for the problem of cosmological acceleration of inhomogeneities with sub-horizon characteristic scales today. Because of the significant growth of such inhomogeneities at recent times, a perturbative treatment may not be sufficient. An exact solution of the Einstein equations, even for a simplified geometry, could be more useful in order to reveal an underlying mechanism. The Tolman-Bondi metric [6] has been employed often in this context [7]–[12]. It has been observed that any form of the luminosity distance as a function of the redshift can be reproduced with this metric [10].

A drawback of the standard handling of the Tolman-Bondi metric is that the radial coordinate is defined such that the fluid density is initially perceived as homogeneous. The presence of inhomogeneities is introduced through a function that determines the local Big Bang time. This obscures the intuition on the role of large mass concentrations. Moreover, the growth of perturbations and its effect on the expansion is not obvious.

In our analysis we choose a gauge such that the initial density perturbation is apparent. We first model the perturbation by matching a Schwarzschild metric in the interior with an exterior Tolman-Bondi metric. We show that the presence of a large overdensity modifies the cosmological evolution of the surrounding fluid. In particular, accelerating expansion can take place along the radial direction and can be observed through the redshift of light signals propagating radially. On the other hand, the expansion perpendicularly to the radial direction is characterized by deceleration.

Underdensities do not induce acceleration in any direction.

As an exotic possibility, we also consider the case of a negative mass at the center. A fluid with energy density that can become negative has already been discussed in the literature. In ref. [13] a field termed phantom with negative kinetic energy drives the accelerating expansion. Our setup is based on less drastic assumptions. We consider vacuum solutions of the Einstein equations that can be interpreted as arising from objects of negative mass. The relevant metric is the Schwarzschild one with a negative mass. We show that a pressureless fluid near the center of such a configuration can have accelerating expansion perpendicularly to the radial direction.

We should mention at this point that negative-mass configurations have several features that appear problematic, and their physical significance is not guaranteed. The negative-mass Schwarzschild solution has a naked singularity at the center, so that it violates the cosmic censorship conjecture. However, naked singularities appear often in studies of gravitational collapse for large classes of initial conditions [14]. Another issue concerns the stability of the negative-mass Schwarzschild solution, which has not been proven in full generality. In ref. [16] the linear stability has been demonstrated, under a family of boundary conditions at the singularity that have a physical motivation. On the other hand, runaway solutions of the Einstein equations are known for a pair of objects with positive and negative mass [15, 16]. We do not offer here a resolution of these problematic issues. Instead, we point out an interesting feature of the negative-mass Schwarzschild solution related to the issue of the cosmological acceleration.

Next we consider a homogeneous energy distribution in the central region. We define an initial condition for the spatial curvature which makes our model very similar to that of spherical collapse [17]. A small overdensity grows consistently with the perturbative Jeans analysis, until the density fluctuation becomes comparable to the average density. Then, the overdensity starts collapsing. We study the null geodesics that start outside the perturbation and lead to an observer in its interior. If the observer is located in the center of the spherical perturbation the geodesics follow the radial direction. The accelerated expansion of the surrounding fluid is reflected in their form, which, in turn, determines the luminosity distance of a light source as a function of the redshift.

We demonstrate that the expected luminosity distance is consistent with accelerated expansion for a certain range of redshifts. In this work we do not put emphasis on the exact numerical consistency with the data. The reason is that we model the fluid in the central collapsing region as pressureless. This results in a strong deceleration for small redshifts, which is not expected to be present if the cosmological fluid can reach virialization. Our main point is the identification of a mechanism that could drive the observed acceleration. This mechanism is based on the gravitational force that acts on the fluid surrounding a collapsing overdensity and its effect on the expansion rate.

In the following section we discuss the cosmological expansion in inhomogeneous

cosmologies and its dependence on the direction of observation. In section 3 we employ the Tolman-Bondi metric in order to construct a model for a central inhomogeneity in an asymptotically homogeneous Universe. In section 4 we examine if acceleration can be induced by the inhomogeneity along or perpendicularly to the radial direction. In section 5 we study the form of the luminosity distance as a function of the redshift for an observer located at the center of an overdensity. In section 6 we provide a summary of the results and our conclusions.

2. Acceleration in inhomogeneous cosmology

The presence of a center in the configuration that we would like to study implies that we have to assume a metric appropriate for an inhomogeneous fluid. Under the assumption of spherical symmetry, the most general metric for a pressureless, inhomogeneous fluid is the Tolman-Bondi metric [6]. It can be written in the form

$$ds^2 = -dt^2 + b^2(t, r)dr^2 + R^2(t, r)d\Omega^2, \quad (2.1)$$

where $d\Omega^2$ is the metric on a two-sphere. The function $b(r, t)$ is given by

$$b^2(t, r) = \frac{R_{,r}^2(t, r)}{1 + f(r)}, \quad (2.2)$$

where the subscript denotes differentiation with respect to r , and $f(r)$ is an arbitrary function. The bulk energy momentum tensor has the form

$$T_B^A = \text{diag}(-\rho(t, r), 0, 0, 0). \quad (2.3)$$

The fluid consists of successive shells marked by r , whose local density ρ is time-dependent. The function $R(t, r)$ describes the location of the shell marked by r at the time t . Through an appropriate rescaling it can be chosen to satisfy [14]

$$R(0, r) = r. \quad (2.4)$$

The Einstein equations reduce to

$$R_{,t}^2(t, r) = \frac{1}{8\pi M^2} \frac{\mathcal{M}(r)}{R} + f(r) \quad (2.5)$$

$$\mathcal{M}_{,r}(r) = 4\pi R^2 \rho R_{,r}, \quad (2.6)$$

with $G = (16\pi M^2)^{-1}$. The generalized mass function $\mathcal{M}(r)$ of the fluid can be chosen arbitrarily. It incorporates the contributions of all shells up to r . It determines the energy density through eq. (2.6). Because of energy conservation $\mathcal{M}(r)$ is independent of t , while ρ and R depend on both t and r .

The volume expansion rate is usually defined through the four-velocity of the fluid u^a as

$$3H = u^a_{;a} = u_{a;b} g^{ab} = u_{a;b} h^{ab}, \quad (2.7)$$

where

$$h^{ab} = g^{ab} + u^a u^b. \quad (2.8)$$

The Raychaudhuri equation constrains its evolution with time. It reads

$$\dot{H} \equiv H_{,c} u^c = -H^2 - \frac{1}{3}\sigma_{ab}\sigma^{ab} + \frac{1}{3}\omega_{ab}\omega^{ab} - \frac{1}{3}R_{ab}u^a u^b, \quad (2.9)$$

where σ_{ab} and ω_{ab} are the shear and vorticity tensors respectively. For an observer comoving with a pressureless and irrotational fluid, the acceleration parameter is

$$q = \frac{\dot{H}}{H^2} + 1 = -\frac{1}{H^2} \left(\frac{1}{3}\sigma_{ab}\sigma^{ab} + \frac{1}{12M^2}\rho \right). \quad (2.10)$$

If the local energy density is positive, no acceleration can take place.

In the context of inhomogeneous cosmology the definition (2.7) does not capture the variation of the expansion rate in different directions. For example, the Tolman-Bondi (2.1) has a preferred direction (the radial one). In such situations we can define a tensor p^{ab} that projects every quantity perpendicularly to the preferred space-like direction s^a (and of course the time-like vector field u^a). This is

$$p^{ab} = g^{ab} + u^a u^b - s^a s^b = h^{ab} - s^a s^b. \quad (2.11)$$

For the Tolman-Bondi metric (2.1) we have $s^a = b^{-1}\partial_r$. We can now define invariant expansion rates parallel and perpendicularly to s^a , according to [8]

$$H_r = u_{a;b} s^a s^b = \frac{b_{,t}}{b} = \frac{R_{,rt}}{R_{,r}} \quad (2.12)$$

$$H_\theta = \frac{1}{2}u_{a;b} p^{ab} = \frac{R_{,t}}{R}, \quad (2.13)$$

so that

$$H = \frac{2}{3}H_\theta + \frac{1}{3}H_r. \quad (2.14)$$

From the above, it is obvious that H corresponds to an average of the expansion rates in various directions. If the acceleration is defined through H , the expansion is always decelerating for $\rho > 0$. This is the conclusion drawn in previous studies [7, 8, 9]. However, it is possible that the expansion may be accelerating in some direction even though eq. (2.10) always holds.

A definition of the expansion rate that takes into account its directional dependence is given in ref. [19]. It is

$$\hat{H} = \frac{1}{3}u^a_{;a} + \sigma_{ab}J^a J^b, \quad (2.15)$$

where σ_{ab} is the shear tensor and J^a a unit vector pointing in the direction of observation. In the context of the Tolman-Bondi metric, and for an observer located away from the center of the configuration, the above definition gives [19]

$$\hat{H} = \frac{R_{,t}}{R} + \left(\frac{b_{,t}}{b} - \frac{R_{,t}}{R} \right) \cos^2 \psi. \quad (2.16)$$

The parameter ψ is the angle between the radial direction through the observer and the direction of observation. For $\psi = 0$ or π we have $\hat{H} = H_r$, while for $\psi = \pi/2$ or $3\pi/2$ we have $\hat{H} = H_\theta$.

A definition of the acceleration parameter in a specific direction can be given in terms of the expansion of the luminosity distance D_L of a light source in powers of the redshift z of the incoming photons. For small z this is

$$\hat{q} = \hat{H} \frac{d^2 D_L}{dz^2} - 1. \quad (2.17)$$

In ref. [19] the acceleration parameter was calculated in the context of the Tolman-Bondi metric for an observer located away from the center of spherical symmetry. The result is [19]

$$\hat{q} = \frac{1}{\hat{H}^2} \left(C_3 + C_4 |\cos \psi| + C_5 \cos^2 \psi + C_6 |\cos \psi|^3 \right) + 3 \quad (2.18)$$

$$C_3 = \frac{R_{,tt}}{R} - 3 \frac{R_{,t}^2}{R^2} \quad (2.19)$$

$$C_4 = 3\sqrt{1+f} \left(\frac{R_{,t}}{R^2} - \frac{R_{,tr}}{R_r R} \right) \quad (2.20)$$

$$C_5 = 3 \frac{R_{,t}^2}{R^2} - 3 \frac{R_{,tr}^2}{R_{,r}^2} - \frac{R_{,tt}}{R} + \frac{R_{,ttr}}{R_{,r}} \quad (2.21)$$

$$C_6 = \sqrt{1+f} \left(3 \frac{R_{,tr}}{R R_{,r}} + \frac{R_{,tr} R_{,rr}}{R_{,r}^3} - 3 \frac{R_{,t}}{R^2} - \frac{R_{,trr}}{R_{,r}^2} \right). \quad (2.22)$$

For $\psi = 0$ or π and $\psi = \pi/2$ or $3\pi/2$ the acceleration is, respectively,

$$q_r = \left(\frac{b}{b_{,t}} \right)^2 \left[\frac{b_{,tt}}{b} - \frac{1}{b} \left(\frac{b_{,t}}{b} \right)_{,r} \right], \quad (2.23)$$

$$q_\theta = \left(\frac{R}{R_{,t}} \right)^2 \frac{R_{,tt}}{R}. \quad (2.24)$$

These parameters do not depend solely on local quantities, as opposed to the acceleration parameter of eq. (2.10). For example, from eq. (2.5) we have

$$q_\theta = -\frac{1}{16\pi M^2} \frac{\mathcal{M}}{R^3} \frac{1}{H_\theta^2}. \quad (2.25)$$

The value of q_θ depends on the total mass function and not just the local energy density. For $\mathcal{M} > 0$ we expect to observe deceleration perpendicularly to the radial direction, while for $\mathcal{M} < 0$ acceleration.

It must be emphasized that the expressions (2.23), (2.24) refer to the effective acceleration deduced from light signals that originate in the vicinity of an off-center observer. In this sense, they determine the character of the local expansion. It is interesting that they do not predict a dipole component [19]. On the other hand, light

signals that travel longer distances (e.g. from outside a spherical inhomogeneity to its center) integrate information on the local expansion along their whole trajectory. We shall discuss the form of the luminosity distance as a function of the redshift for this case in a following section.

Finally, we point out that in the standard treatment of the Tolman-Bondi metric [7]–[12] the radial coordinate is taken such that the initial energy density is perceived as homogeneous. Moreover, the function $f(r)$ is assumed to be zero in order to provide consistency with a matter dominated, flat Universe. The inhomogeneity is introduced through a function $t_b(r)$ that appears in the integration of the Friedmann equation and determines the local Big Band time. Our approach is closer to the physical picture, as the overdensities are apparent from the beginning. Moreover, we put the emphasis on their effect on the cosmological evolution of the surrounding fluid.

3. Expansion near an inhomogeneity

We would like to describe the cosmological evolution around a central region in which the mass function deviates from the form implied by a homogeneous distribution of matter. We have in mind the general form

$$\mathcal{M}(r) = \mathcal{M}_0 + \delta\mathcal{M}(r), \quad (3.1)$$

with \mathcal{M}_0 positive or negative. Even for negative \mathcal{M}_0 we assume that eq. (2.6) is satisfied with $\rho \geq 0$. No negative energy density appears in the energy-momentum tensor, and the weak energy condition holds. We now have

$$\delta\mathcal{M}_{,r} = 4\pi S^2 \rho S_{,r}. \quad (3.2)$$

The most convenient way to realize our scenario is by matching two spherically symmetric space-times. We assume that in the central region the metric takes the Schwarzschild form with mass \mathcal{M}_0

$$ds^2 = -A^2(\tilde{r})d\tilde{t}^2 + B^2(\tilde{r})d\tilde{r}^2 + \tilde{r}^2d\Omega^2, \quad (3.3)$$

where $A^2(\tilde{r}) = B^{-2}(\tilde{r}) = 1 - \mathcal{M}_0/(8\pi M^2\tilde{r})$. The Tolman-Bondi metric (2.1) determines the geometry at large distances. The two regions are separated by a spherical surface with metric

$$ds^2 = -d\tau^2 + S^2(\tau)d\Omega^2. \quad (3.4)$$

The physical situation described by our scenario does not involve necessarily a singularity at the origin. For $\mathcal{M}_0 > 0$ the metric of eq. (3.3) may result from a compact object with positive energy density and radius smaller than $S(\tau)$. For $\mathcal{M}_0 < 0$ we are forced to consider eq. (3.3) as a vacuum solution in order to avoid a negative energy density.

The matching of (2.1) and (3.4) leads to

$$S^2(\tau) = R^2(t(\tau), r(\tau)) \quad (3.5)$$

$$-\dot{t}^2(\tau) + b^2(t(\tau), r(\tau)) \dot{r}^2(\tau) = -1, \quad (3.6)$$

where a dot denotes a derivative with respect to the proper time τ on the surface. The matching of (3.3) and (3.4) gives

$$S^2(\tau) = \tilde{r}^2(\tau) \quad (3.7)$$

$$-A^2(\tilde{r}(\tau)) \dot{\tilde{t}}^2(\tau) + B^2(\tilde{r}(\tau)) \dot{\tilde{r}}^2(\tau) = -1. \quad (3.8)$$

The absence of shell crossing implies $\dot{r}(\tau) = 0$. The shell that coincides with the matching surface is always the same. As a result, it maintains a constant value $r(\tau) = r_0$. Eq. (3.6) then gives $t(\tau) = \tau$, while eq. (3.5) can be written as $S(\tau) = R(\tau, r_0)$.

In order to obtain an equation for $S(\tau)$ we need the additional assumption that there is no singular energy density on the matching surface. This implies that the extrinsic curvature is continuous across the surface. The resulting condition reads

$$S(\tau) \left(\dot{S}^2(\tau) + \frac{1}{B^2(S(\tau))} \right)^{1/2} = \frac{R(\tau, r_0) R_{,r}(\tau, r_0)}{b(\tau, r_0)}. \quad (3.9)$$

Making use of eq. (2.2) we find

$$\dot{S}^2(\tau) = f(r_0) + \frac{1}{8\pi M^2} \frac{\mathcal{M}_0}{S(\tau)}. \quad (3.10)$$

This coincides with the equation of motion of the first shell, as derived from eqs. (2.5), (2.6).

We can conclude that, in the absence of shell crossing, the interior Schwarzschild metric can be matched with the exterior Tolman-Bondi one on a spherical surface that coincides with the location of the first shell $S(\tau, r_0)$. The equation of motion for the shells of fluid is

$$\frac{\dot{R}^2(\tau, r)}{R^2} = \frac{1}{8\pi M^2} \frac{\mathcal{M}(r)}{R^3} + \frac{f(r)}{R^2}, \quad (3.11)$$

where $\mathcal{M}(r)$ is given by eq. (3.1) with $\delta\mathcal{M}(r) \rightarrow 0$ for $r \rightarrow r_0$. The initial condition is given by eq. (2.4). The above equation can be considered as a generalization of the standard Friedmann equation for an inhomogeneous cosmological fluid. The integrated mass within a spherical volume of comoving radius r is given by $\mathcal{M}(r)$, while the function $f(r)$ defines a generalized curvature term.

In order for eq. (2.5) to have a solution, the two arbitrary functions $f(r)$ and $\mathcal{M}(r)$ must satisfy $f(r) \geq -\mathcal{M}(r)/(8\pi M^2 r)$ for all r . The function $f(r)$ defines an effective curvature term in eq. (2.5). We can also interpret $f(r)$ as part of the initial radial velocity of the fluid. This has to be non-zero in the presence of a negative mass for a physically meaningful solution to exist.

As a physically motivated example we consider a fluid with energy density that is initially constant for $r \geq r_0$, so that $\delta\mathcal{M}(r) = 4\pi\rho_0(r^3 - r_0^3)/3$. We assume that a spherically symmetric inhomogeneity has appeared during the cosmological evolution of the fluid (probably as a result of gravitational instability). At $t_i = 0$ the inhomogeneity is concentrated in the region $r < r_0$. We parametrize the total mass of the inhomogeneity as $\mathcal{M}_0 = 4\pi\rho r_0^3/3$ with $\rho = \epsilon\rho_0$. For $\epsilon > 1$ the inhomogeneity is a local overdensity, for $0 \leq \epsilon < 1$ an underdensity, while for $\epsilon < 0$ we have an object of negative mass at the center of the configuration.

Our crucial assumption is that the expansion rate at some initial time t_i is given for all r by the standard expression in homogeneous cosmology: $H_i^2 = \rho_0/(6M^2)$. We essentially assume that the expansion is completely homogeneous at the time of appearance of the inhomogeneity. This is very similar to the initial condition considered within the context of the model of spherical collapse [17, 18]. Then, eq. (3.11) with $R(0, r) = r$ implies that $\bar{f}(\bar{r}) = (1 - \epsilon)/\bar{r}$, where $\bar{f} = f/\bar{H}_i^2$ and $\bar{H}_i = H_i r_0$. An effective curvature term appears that is proportional to the size of the inhomogeneity $\epsilon - 1$. For $\bar{r} \rightarrow \infty$ we have $\bar{f} \rightarrow 0$, so that the curvature term disappears and we recover the standard expansion in a spatially flat Universe.

Eq. (3.11) can be written as

$$\frac{\dot{\bar{R}}^2}{\bar{R}}(\bar{\tau}, \bar{r}) = \frac{\epsilon - 1 + \bar{r}^3}{\bar{R}} + \frac{1 - \epsilon}{\bar{r}}, \quad (3.12)$$

where $\bar{\tau} = tH_i = \tau H_i$, $\bar{R} = R/r_0$, $\bar{r} = r/r_0$, and the dot denotes a derivative with respect to $\bar{\tau}$. Sufficiently far from the center of the configuration (large \bar{r}), eq. (3.12) reduces to the standard Friedmann equation for a homogeneous, matter dominated, flat Universe: $(\dot{\bar{R}}/\bar{R})^2 \sim \bar{R}^{-3}$. Near the center of the configuration the expansion is inhomogeneous.

For the value $\epsilon = 1$ we recover the standard homogeneous expansion. In this case the total mass in the region $\bar{r} < 1$ could arise from a fluid with constant initial energy density equal to ρ_0 . The range $\epsilon > 1$ corresponds to an overdensity in the region $\bar{r} < 1$. This could result from a continuous distribution of matter, or from a singularity at the center, such as a black hole. The range $0 \leq \epsilon < 1$ corresponds to an underdensity. Finally, the range $\epsilon < 0$ corresponds to a negative mass at the center.

In the case of an overdensity ($\epsilon > 1$), there is a certain time $\bar{\tau}_c$ when $\bar{R}(\bar{\tau}_c, 1)$ is sufficiently large for the r.h.s. of eq. (3.12) to vanish at $\bar{r} = 1$. At later times the first shell must reverse its motion and contract. This is very similar to the phase of collapse in the spherical collapse model.

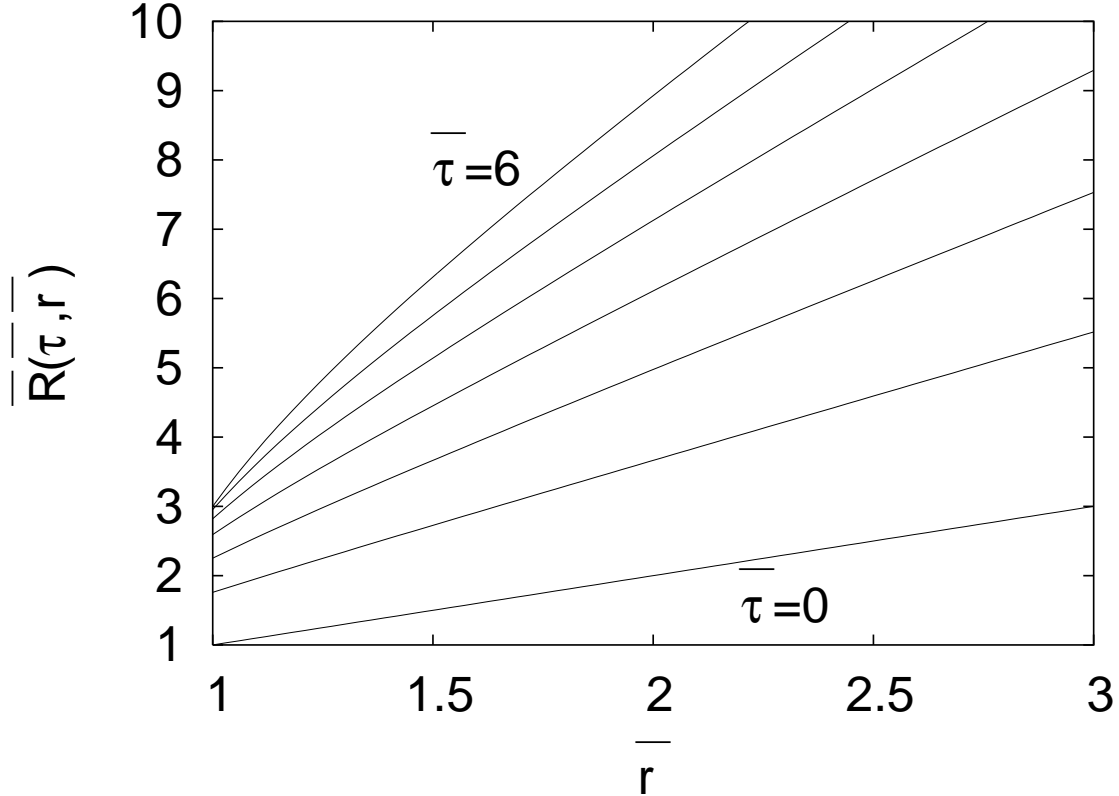


Figure 1. The solution $\bar{R}(\bar{\tau}, \bar{r})$ of eq. (3.12) for $\epsilon = 1.5$.

4. The local acceleration

4.1. Positive mass

In fig. 1 we plot the solution of eq. (3.12) for $\epsilon = 1.5$, with the initial condition $\bar{R}(0, \bar{r}) = \bar{r}$. We observe deviations from the initial linear relation between $\bar{R}(\bar{\tau}, \bar{r})$ and \bar{r} . These are induced by the overdensity at $\bar{r} < 1$. In particular, the additional gravitational attraction on the shells with $\bar{r} \simeq 1$, resulting from the overdensity, slows down the outward motion of these shells. At times $\bar{\tau} \sim 6$ the first shell is beginning to reverse its motion and collapse towards the center. The fluid far from the overdensity is not affected significantly by it. Its expansion is typical of a homogeneous fluid.

The evolution in fig. 1 is very similar to the one observed in the spherical collapse model [17]. An initial overdensity decouples from the homogeneous expansion and eventually reverses its motion and collapses. Our model provides additional information on the evolution of the material that surrounds such an overdensity. In particular, the relative motion of two fluid shells can be determined. It is apparent from fig. 1 that the \bar{r} -derivative of the function $\bar{R}(\bar{\tau}, \bar{r})$ is largest near $\bar{r} = 1$. This implies that the relative

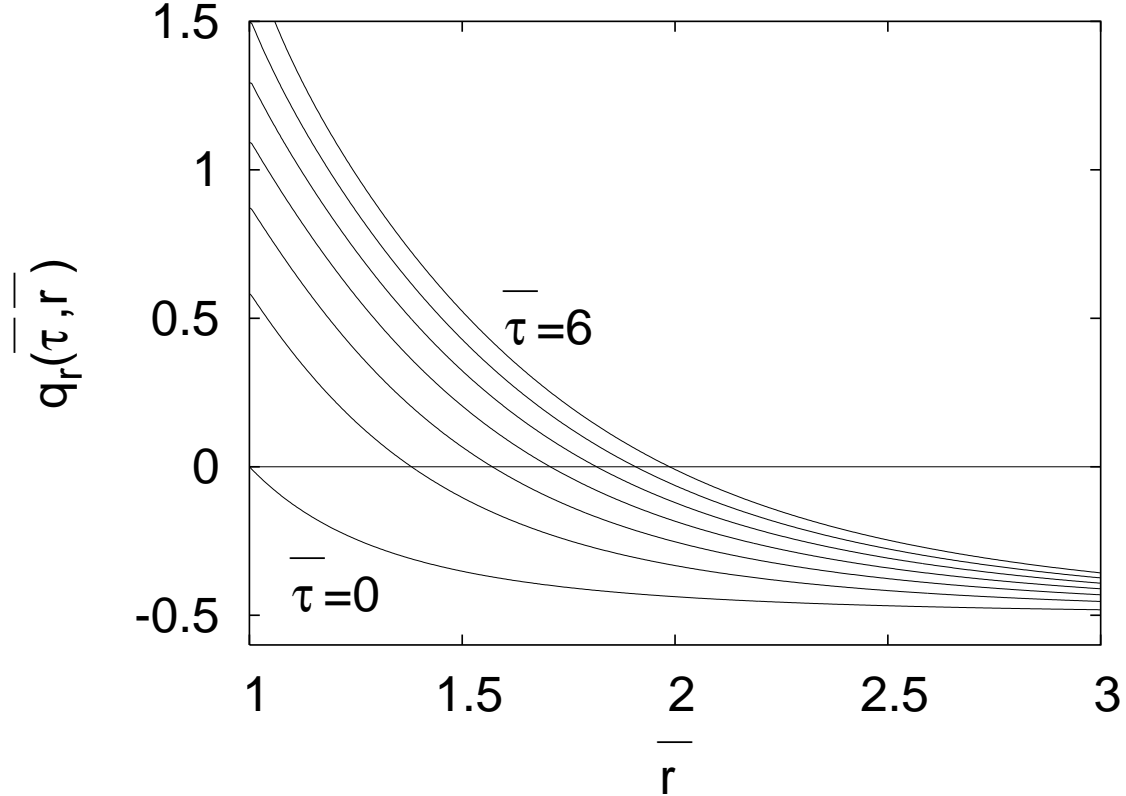


Figure 2. The local acceleration parameter $q_r(\bar{\tau}, \bar{r})$ in the radial direction for $\epsilon = 1.5$.

separation of the shells nearest to the center increases in comparison to the unperturbed fluid at large \bar{r} . For a comoving observer with $\bar{r} \simeq 1$ the expansion seems faster than in the homogeneous model. On the other hand, two observers with the same radial distance from the center, but located at different angles, have a relative separation that tends to increase at a slower rate than for a homogeneous fluid.

This behaviour is reflected in the values of the acceleration parameters. They can be expressed as

$$q_r = \left(\frac{\bar{b}}{\dot{\bar{b}}} \right)^2 \left[\frac{\ddot{\bar{b}}}{\bar{b}} - \frac{1}{\bar{b}} \left(\frac{\dot{\bar{b}}}{\bar{b}} \right)' \right], \quad (4.1)$$

$$q_\theta = \left(\frac{\bar{R}}{\dot{\bar{R}}} \right)^2 \frac{\ddot{\bar{R}}}{\bar{R}}, \quad (4.2)$$

where $\bar{b} = \bar{R}' / \sqrt{\bar{H}_i^{-2} + \bar{f}}$, $\bar{f} = f / \bar{H}_i^2$, $\bar{H}_i = H_i r_0$, the dot denotes a derivative with respect to $\bar{\tau}$, and the prime a derivative with respect to \bar{r} . We use $\bar{H}_i = 1$ throughout this section. The parameter $q_r(\bar{\tau}, \bar{r})$ in the radial direction is plotted in fig. 2. Initially it is negative for all \bar{r} . At later times it becomes positive in the central region. At all times

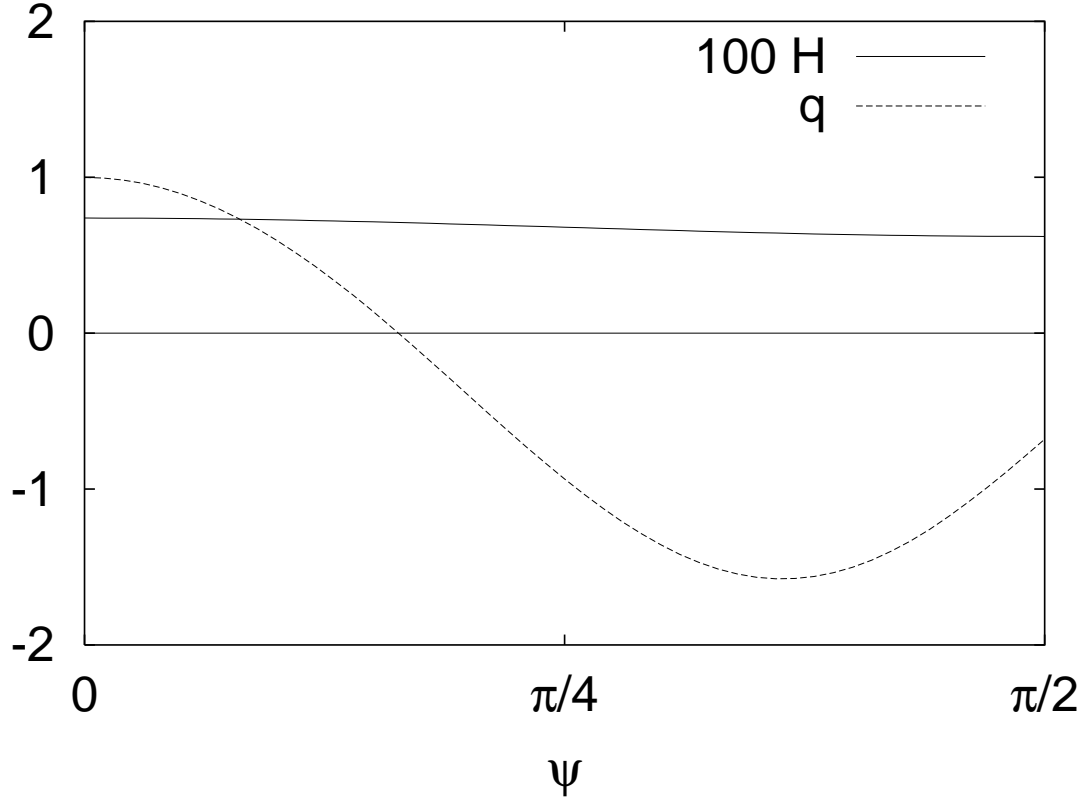


Figure 3. The expansion rate \hat{H} and the local acceleration parameter \hat{q} , as a function of the angle ψ relative to the radial direction, for $\epsilon = 1.01$, $\bar{r} = 1$ and $\bar{\tau} = 100$.

and for large \bar{r} it approaches asymptotically the value $q_r = -0.5$, typical of a homogenous matter-dominated flat Universe. The acceleration parameter $q_\theta(\bar{\tau}, \bar{r})$ perpendicularly to the radial direction is always negative. For large \bar{r} it approaches the value $q_\theta = -0.5$ as well.

The appearance of accelerating expansion does not require $\epsilon \gg 1$ necessarily. In fig. 3 we plot the expansion rate \hat{H} and the acceleration \hat{q} as a function of the angle ψ for a model with $\epsilon = 1.01$. For this we employ the expressions (2.16) and (2.18)–(2.22). We consider the first shell with $\bar{r} = 1$ at a time $\bar{\tau} = 100$. The dependence of the expansion rate on the angle is mild. We can observe signs of the slowing down of the relative expansion perpendicularly to the radial direction: $H_\theta \equiv \hat{H}(\pi/2) < H_r \equiv \hat{H}(0)$. On the other hand, the system is far from the period of collapse, which will take place at times $\bar{\tau} = \mathcal{O}(10^3)$. At $\bar{\tau} = 100$ the ratio of the average density in the region $r < r_0$ and the density at large r is $\rho_0/\rho_\infty \simeq [(R_\infty/r_\infty)/(R_0/r_0)]^3 \epsilon \simeq 1.18$. The local overdensity can still be considered a perturbation of the homogeneous background. Despite that, it induces an effective acceleration close to the radial direction, for angles $\psi \lesssim \pi/6$.

For $0 \leq \epsilon \leq 1$ both acceleration parameters remain negative at all times. This means

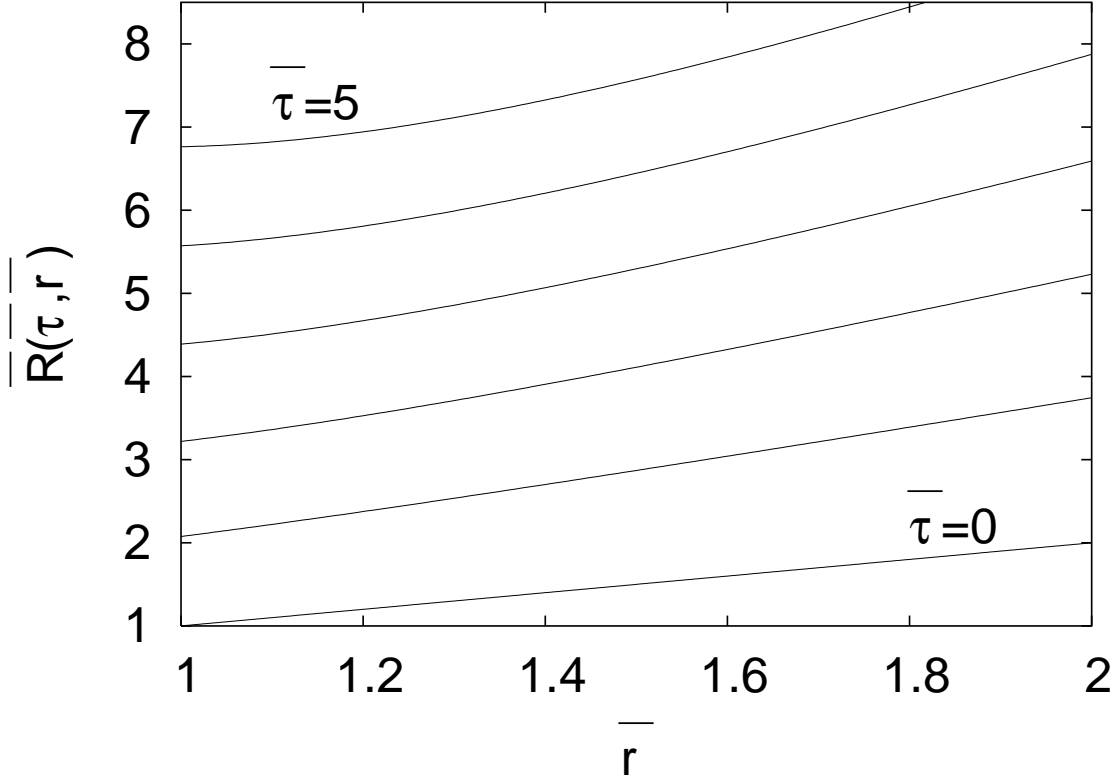


Figure 4. The solution $\bar{R}(\bar{\tau}, \bar{r})$ of eq. (3.12) for $\epsilon = -0.5$.

that the presence of a void cannot induce accelerating expansion in the neighbouring regions.

4.2. Negative mass

In fig. 4 we plot the solution of eq. (3.12) for $\epsilon = -0.5$, with the initial condition $\bar{R}(0, \bar{r}) = \bar{r}$. As in fig. 1, we observe deviations from the initial linear relation between $\bar{R}(\bar{\tau}, \bar{r})$ and \bar{r} . In this case, however, the shells nearest to the center are repelled strongly by the negative mass. They expand faster than the unperturbed medium at large \bar{r} . At times $\bar{\tau} \simeq 5$ the first shell catches up with the adjacent one (the \bar{r} -derivative of $\bar{R}(\bar{\tau}, \bar{r})$ vanishes at $\bar{r} = 1$) and the phenomenon of shell crossing appears. This is caused by the absence of pressure in our approximation. Our model is not adequate for the discussion of the evolution at later times.

For $0 \leq \bar{\tau} \lesssim 1$ the relative separation of adjacent shells near $\bar{r} = 1$ increases, but with a decreasing rate. This is reflected in the negative value of the acceleration parameter $q_r(\bar{\tau}, \bar{r})$. For $\bar{\tau} \gtrsim 1$ the relative separation decreases. As a consequence, an observer comoving with the fluid should perceive contraction in the radial direction. This

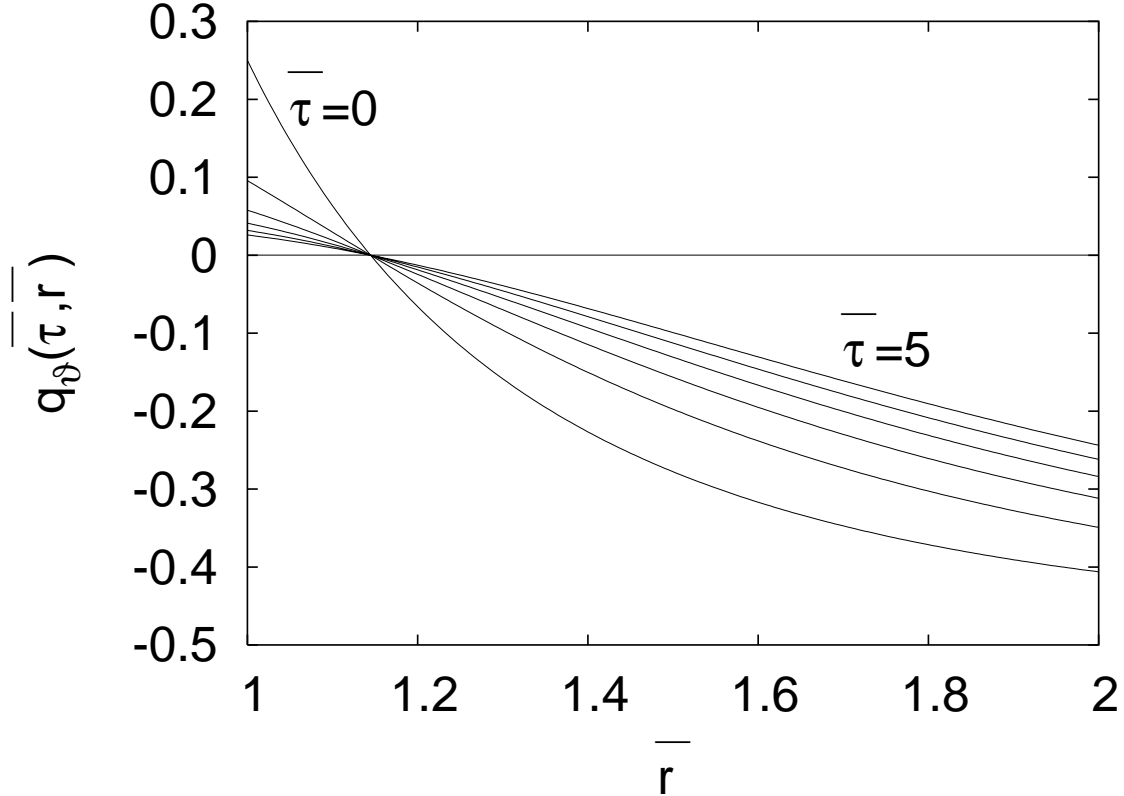


Figure 5. The local acceleration parameter $q_\theta(\bar{\tau}, \bar{r})$ perpendicularly to the radial direction for $\epsilon = -0.5$.

is confirmed by the value of the expansion rate H_r of eq. (2.12), which becomes negative for $\bar{\tau} \gtrsim 1$ near $\bar{r} = 1$. On the other hand, the relative separation of two observers with the same \bar{r} , but located at different angles, increases faster near $\bar{r} = 1$ than for large \bar{r} . The acceleration parameter $q_\theta(\bar{\tau}, \bar{r})$ perpendicularly to the radial direction is plotted in fig. 5. From eq. (3.12) we find

$$\frac{d^2 \bar{R}}{d \bar{\tau}^2} = -\frac{\epsilon - 1 + \bar{r}^3}{2 \bar{R}^2}. \quad (4.3)$$

This implies that $q_\theta(\bar{\tau}, \bar{r})$ is positive for $\bar{r} < 1.5^{1/3} \simeq 1.15$ at all times for our choice of parameters. For large \bar{r} both acceleration parameter approach asymptotically the value $q = -0.5$, typical of a homogenous matter-dominated flat Universe.

5. The luminosity function for a central observer

In this section we would like to study the issue of accelerated expansion for an observer within the perturbation. We assume that the observer is located at the center of a spherically symmetric overdensity and receives light signals from distances that extend

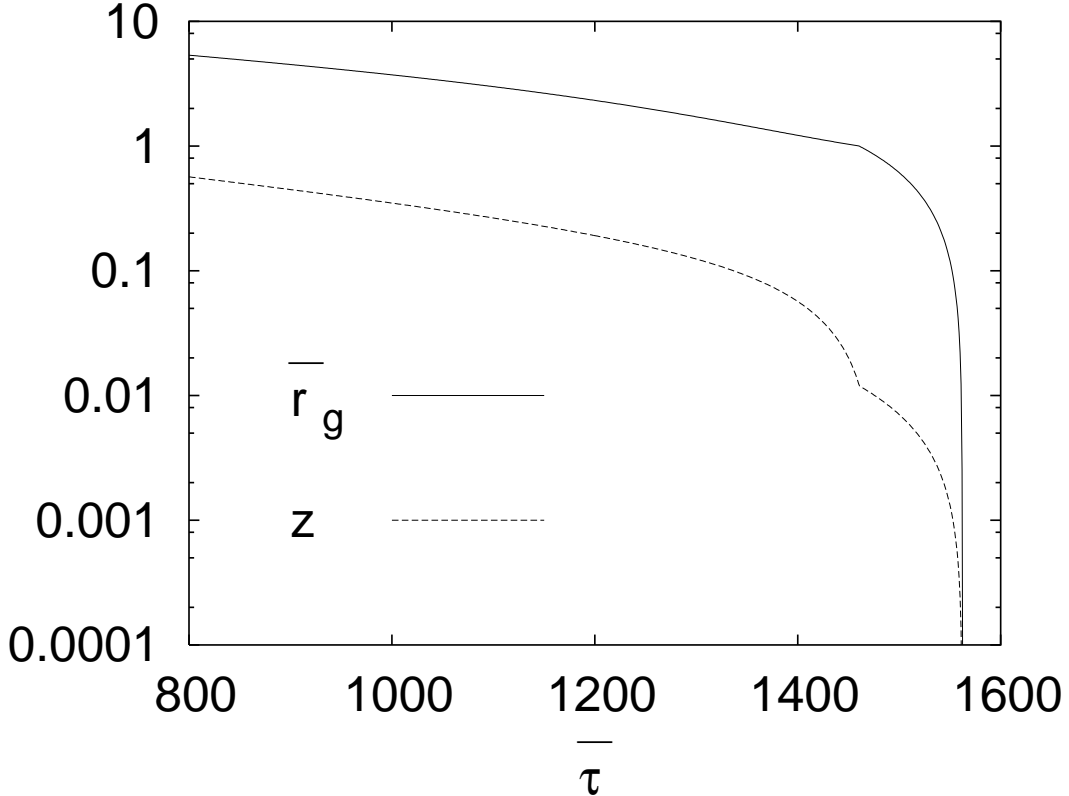


Figure 6. The null geodesic $\bar{r}_g(\bar{\tau})$ and the redshift $z(\bar{\tau})$ for a model with $\epsilon = 1.01$, $\bar{H}_i = 1$, $\bar{\tau}_e = 1461$, $\bar{\tau}_0 = 1563$.

beyond its surface. The assumption of spherical symmetry makes the problem tractable. In a realistic scenario we expect deviations from the exact symmetry, but the essence of the mechanism should remain unaffected. On the other hand, the preferred location of the observer is a more profound assumption. It could be argued that we are located near the center of a galaxy, which is a significant perturbation in the average density. However, it is questionable if an effect at the galactic scale can leave traces in the expansion at the level of the horizon. On the other hand, the mechanism we consider may be relevant for inhomogeneous cosmologies with many centers. The study of this situation is very difficult technically, and some kind of averaging will have to be implemented. The necessary formalism in order to address this problem has not been developed yet.

The other important feature of the scenario with an observer at the center of symmetry is that all the incoming signals follow radial geodesics. The radial acceleration can become positive, in contrast to the tangential one. In this sense, the central location of the observer provides the optimum scenario for our purposes.

We also mention that our assumption about the location of the observer provides automatic consistency with the isotropy of the cosmic microwave background. Deviations

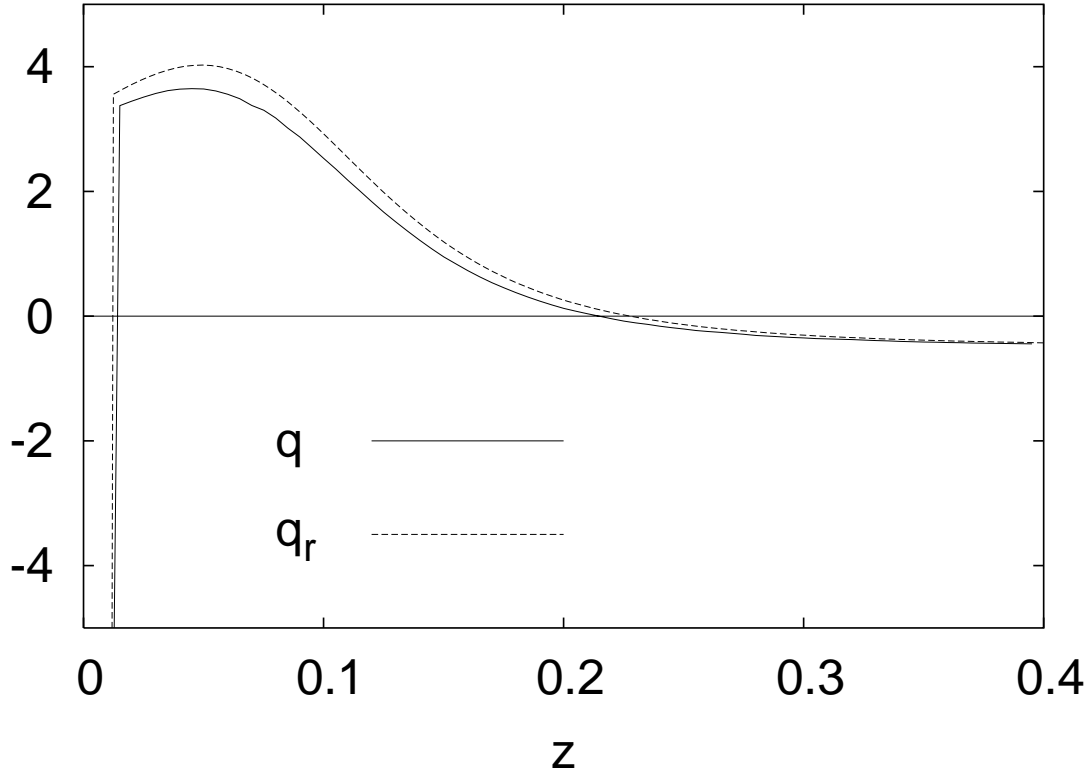


Figure 7. The acceleration parameter q and the local radial acceleration q_r as a function of the redshift z , for a model with $\epsilon = 1.01$, $\bar{H}_i = 1$, $\bar{\tau}_0 = 1563$, $z_0 = 0.012$.

from complete isotropy, as quantified in the difference of power between the northern and southern hemisphere or possible alignments of the low multipoles [20], could possibly allow for an off-center location as well. An alternative possibility is that the isotropy appears at a sufficiently large length scale in a configuration with several centers of symmetry. It remains to be seen if the radial acceleration can be the dominant contribution for a random location of the observer.

The simplest example of a perturbation on a homogeneous background has

$$\rho = \epsilon \rho_0 \quad \text{for } r \leq r_0 \quad (5.1)$$

$$\rho = \rho_0 \quad \text{for } r > r_0. \quad (5.2)$$

The curvature term is

$$\bar{f} = (1 - \epsilon) \bar{r}^2 \quad \text{for } \bar{r} \leq 1 \quad (5.3)$$

$$\bar{f} = \frac{1 - \epsilon}{\bar{r}} \quad \text{for } \bar{r} > 1. \quad (5.4)$$

For $\epsilon > 1$ the inhomogeneity is a local overdensity, for $0 \leq \epsilon < 1$ an underdensity, while

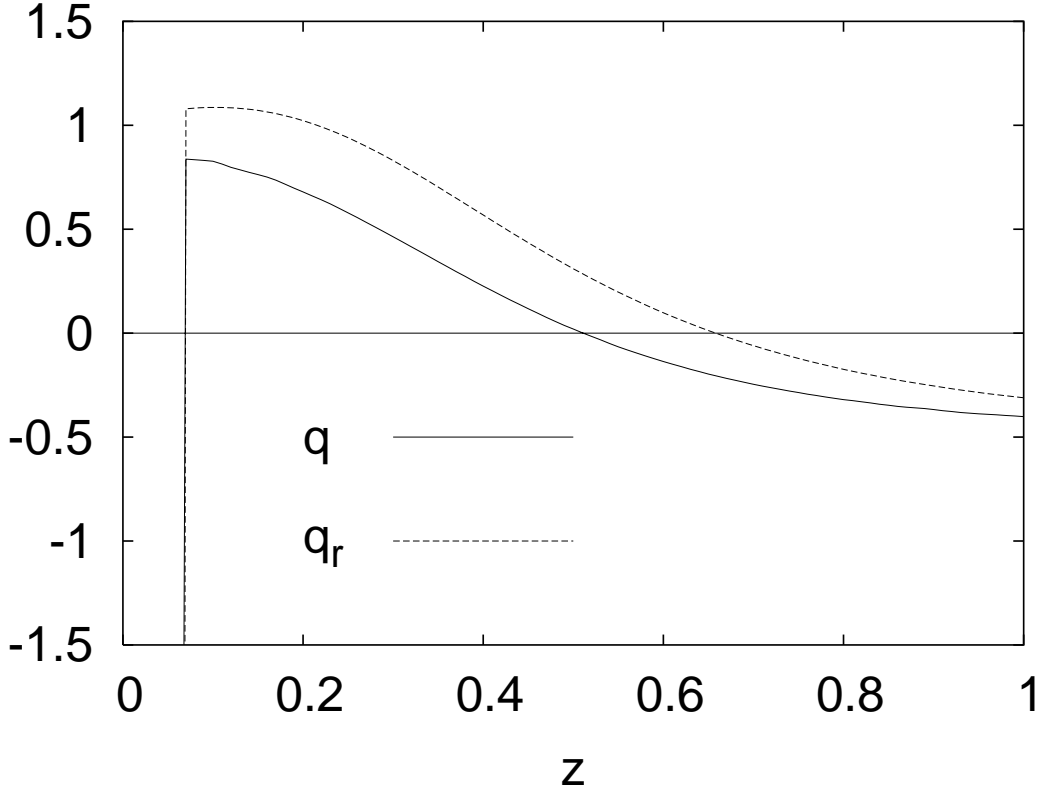


Figure 8. The acceleration parameter q and the local radial acceleration q_r as a function of the redshift z , for a model with $\epsilon = 1.01$, $\bar{H}_i = 4$, $\bar{\tau}_0 = 1567$, $z_0 = 0.067$.

for $\epsilon = 1$ we have a homogeneous energy distribution. The Friedmann equation becomes

$$\frac{\dot{\bar{R}}^2}{\bar{R}^2} = \epsilon \frac{\bar{r}^3}{\bar{R}^3} + (1 - \epsilon) \frac{\bar{r}^2}{\bar{R}^2} \quad \text{for } \bar{r} \leq 1 \quad (5.5)$$

$$\frac{\dot{\bar{R}}^2}{\bar{R}^2} = \frac{\epsilon - 1 + \bar{r}^3}{\bar{R}^3} + \frac{1 - \epsilon}{\bar{r} \bar{R}^2} \quad \text{for } \bar{r} > 1, \quad (5.6)$$

where the dot denotes a partial derivative with respect to $\bar{\tau} = tH_i$. For $\epsilon = 1$ we recover the standard equation for a homogeneous, matter dominated, flat Universe. For $\epsilon > 1$ the interior ($\bar{r} \leq 1$) expands as a homogeneous, closed Universe with spatial curvature proportional to $\epsilon - 1$. The exterior ($\bar{r} > 1$) is inhomogeneous. For large \bar{r} we recover the Friedmann equation for a homogeneous, matter dominated, flat Universe:

$$\frac{\dot{\bar{R}}^2}{\bar{R}^2} = \frac{\bar{r}^3}{\bar{R}^3}. \quad (5.7)$$

We can obtain an analytical expression for the growth of an overdensity in our model. We define the quantity

$$\zeta(\bar{\tau}) = \frac{\bar{R}(\bar{\tau}, \bar{r}_\infty)/\bar{r}_\infty}{\bar{R}(\bar{\tau}, 1)} - 1, \quad (5.8)$$

with $\bar{r}_\infty \gg \bar{r}_0 = 1$. The ratio of the energy density within the perturbation to the energy density far from it is given by the factor $(1 + \zeta)^3$. Using eqs. (5.5), (5.7) we find for $\zeta \lesssim 1$ and $\bar{\tau} \gtrsim 1$

$$\zeta \simeq \frac{\delta}{5} \left(\frac{3}{2} \bar{\tau} \right)^{2/3}, \quad (5.9)$$

where $\delta = \epsilon - 1$. At a time $\bar{\tau}_2 \simeq \delta^{-3/2}$ we have $(1 + \zeta)^3 \simeq 2$, which means that the energy density within the perturbation is double the asymptotic value. The phase of gravitational collapse starts at a time $\bar{\tau}_c \simeq 1.5 \bar{\tau}_2$. The growth of a perturbation $\sim \bar{\tau}^{2/3}$ is in qualitative agreement with the behaviour predicted by the Jeans analysis for subhorizon perturbations in a matter dominated Universe. It is also consistent with the growth of superhorizon perturbations in the matter dominated era. Our model can be viewed as an exact solution of the Einstein equations that is consistent with the behaviour expected from perturbation theory at all the scales of its applicability. This implies that we can consider values larger than one for the dimensionless quantity $\bar{H}_i = H_i r_0$, for which the initial perturbation extends beyond the horizon.

On radial null geodesics we have $ds^2 = d\Omega^2 = 0$, so that the geodesic equation becomes

$$\frac{d\bar{r}_g(\bar{\tau})}{d\bar{\tau}} = - \frac{[\bar{H}_i^{-2} + \bar{f}(\bar{r}_g(\bar{\tau}))]^{1/2}}{\bar{R}'(\bar{\tau}, \bar{r}_g(\bar{\tau}))}, \quad (5.10)$$

where we have considered an incoming signal and the prime denotes a partial derivative with respect to \bar{r} . We first determine numerically a solution of eqs. (5.5), (5.6) and then use the function $\bar{R}(\bar{\tau}, \bar{r})$ in order to derive a solution of eq. (5.10).

The redshift is given by the expression [10]

$$\ln(1 + z) = \int_0^{\bar{r}_{em}} \frac{\dot{\bar{R}}'[\bar{\tau}(\bar{r}_g), \bar{r}_g]}{[1 + f(\bar{r}_g)]^{1/2}} d\bar{r}_g = \int_{\bar{\tau}_{em}}^{\bar{\tau}_0} \frac{\dot{\bar{R}}'[\bar{\tau}, \bar{r}_g(\bar{\tau})]}{\bar{R}'[\bar{\tau}, \bar{r}_g(\bar{\tau})]} d\bar{\tau}. \quad (5.11)$$

The signal is emitted at a time $\bar{\tau}_{em}$ from a point with comoving coordinate \bar{r}_{em} , and is received at the present time $\bar{\tau}_0$ at $\bar{r} = 0$. The rescaled luminosity distance is [11, 19]

$$\bar{D}_L = (1 + z)^2 \bar{R}(\bar{\tau}_{em}, \bar{r}_{em}). \quad (5.12)$$

Through variation of \bar{r}_{em} we obtain the function $D_L(z) = r_0 \bar{D}_L(z)$. The expansion rate and the acceleration as a function of z can be defined as [1]

$$H(z) = \frac{1 + z}{D'_L(z)} = \frac{1}{r_0} \frac{1 + z}{\bar{D}'_L(z)} \quad (5.13)$$

$$q(z) = D''_L(z) \left[\frac{D'_L(z)}{1 + z} - \frac{D_L(z)}{(1 + z)^2} \right]^{-1} - 1 = \bar{D}''_L(z) \left[\frac{\bar{D}'_L(z)}{1 + z} - \frac{\bar{D}_L(z)}{(1 + z)^2} \right]^{-1} \quad (5.14)$$

where the primes denote derivatives with respect to z .

In fig. 6 we plot the null geodesic $\bar{r}_g(\bar{\tau})$ for a model with $\epsilon = 1.01$ corresponding to a small initial overdensity at the level of 1%. The initial time is $\bar{\tau}_i = 0$. We take $\bar{H}_i = 1$,

so that initially the extent of the overdensity is comparable to the horizon: $r_0 = 1/H_i$. At later times the perturbation becomes subhorizon. It is apparent that the form of the geodesic changes at a time $\bar{\tau}_e = 1461$, when the light enters the central homogeneous region of the overdensity. The endpoint of the geodesic is at $\bar{r} = 0$ at the present time $\bar{\tau}_0 = 1563$. In the same figure we also plot the redshift of photons emitted at a certain time $\bar{\tau}_{em}$ by sources located at the comoving coordinate $\bar{r}_g(\bar{\tau}_{em})$ and observed at the present time $\bar{\tau}_0$ at $\bar{r} = 0$. The redshift of a photon emitted at the surface of the central homogeneous region is $z_0 = 0.012$.

In fig. 7 we depict the cosmological acceleration as a function of the redshift. The solid line is the acceleration parameter evaluated through eq. (5.14) for photons emitted at various points along the geodesic of fig. 6. The dashed line is the local radial acceleration given by eq. (4.1) at the point of emission. We observe strong deceleration for redshifts $z < z_0 = 0.012$. These correspond to emission points within the central homogeneous region that expands like a closed Universe. On the other hand, photons emanating from immediately outside the central region indicate strong acceleration. The acceleration remains positive up to redshifts $z \simeq 0.22$. Asymptotically both acceleration parameters approach the value $q = -0.5$, typical of a flat, matter dominated Universe.

In fig. 8 we repeat the calculation for a model with the same value $\epsilon = 1.01$, but with $\bar{H}_i = 4$. This choice corresponds to a superhorizon initial perturbation, as $r_0 = 4/H_i$. The present time is $\bar{\tau}_0 = 1567$ and the redshift of the surface of the homogeneous region $z_0 = 0.067$. The central region is again strongly decelerating. However, there is a range of redshifts extending up to 0.5 or 0.7, for which q or q_r , respectively, are positive.

The direct comparison of the luminosity curves with the data from supernova observations is not feasible within our model. The reason is the presence of the strong deceleration for low redshifts. We have seen that at times $\bar{\tau}_c \sim 1.5\delta^{-3/2} = 1500$ the central region stops expanding and reverses its motion. On the other hand, the absence of pressure in the Tolman-Bondi fluid does not permit a consistent description of the collapsing phase. Our model combines features characterizing the cosmological expansion at large scales and the growth of inhomogeneities at smaller scales. Its simplicity does not allow for quantitative accuracy in its predictions. However, our results demonstrate the presence of a mechanism that could link the cosmological expansion with the appearance of large overdensities.

6. Summary and conclusions

The notion of accelerating expansion has subtleties in inhomogeneous cosmology. The usual definition of the acceleration parameter in terms of eqs. (2.7)–(2.9) leads to eq. (2.10) for a pressureless and irrotational fluid. As a result the expansion is expected to be always decelerating if the energy density remains positive. It is not clear, however, if the

definition of eq. (2.7) is the most appropriate for the characterization of the expansion. The Hubble parameter H in eq. (2.7) accounts for the volume increase at a given point during the expansion. In the presence of inhomogeneities or anisotropies H results from a certain averaging over the various directions. For the Tolman-Bondi metric this is obvious from eq. (2.14). On the other hand, the nature of the expansion deduced through the observation of light from a certain source in the sky is specific to the direction to that source, and not the average over several directions.

If there are preferred directions in the underlying geometry one can define several expansion parameters. For one preferred direction, such definitions are presented in eqs. (2.12), (2.13), where the explicit expressions are also given for the case of the Tolman-Bondi metric. For an observer located away from the center of the configuration, the local Hubble parameter \hat{H} and the acceleration parameter \hat{q} are functions of the angle between the radial direction and that of observation. These parameters can be evaluated by expanding locally the luminosity distance of an incoming signal in powers of the redshift. They are given by eqs. (2.16) and (2.18)–(2.22), respectively. Such a definition of acceleration seems appropriate for the analysis of signals received from distant supernovae [1] or of the photons of the microwave background [2]. In our study we considered the acceleration parameters q_r , q_θ along the radial direction and perpendicularly to it. They are given by eqs. (2.23), (2.24), respectively.

We examined the effect of a mass located near the center of a configuration on the surrounding cosmological fluid. Our approach is similar in spirit to the model of spherical collapse. We considered a fluid that is initially homogeneous and subject to uniform expansion. At a certain time a spherical inhomogeneity appears at some point in space. Its presence modifies the local gravitational field and distorts the expansion of the surrounding fluid. For an observer located in the vicinity of an inhomogeneity, the perceived local evolution is as follows:

- a) A central overdensity leads to acceleration along the radial direction, and deceleration perpendicularly to it.
- b) A central underdensity leads to deceleration along and perpendicularly to the radial direction.
- c) A negative mass at the center leads to deceleration along the radial direction, and acceleration perpendicularly to it.

In all cases the expansion becomes typical of a homogeneous, dust-dominated Universe far away from the inhomogeneity.

Previous studies of expansion within the Tolman-Bondi model [7]–[12] have focused on the acceleration parameter defined through the volume expansion according to (2.7)–(2.9). This corresponds to a certain average of the expansion rates in various directions, as is obvious from eqs. (2.12)–(2.14). The acceleration defined in this way remains always negative, as expected from eq. (2.10). Also, in previous works the Tolman-Bondi metric

has been studied in a gauge in which the initial energy density is constant in space, while the effect of the inhomogeneity is introduced through a function that determines the local Big Bang time. This obscures the intuition on the effect of large concentrations of mass on the expansion. Our treatment clarifies this point and demonstrates the link between overdensities and radial acceleration.

It is apparent from our discussion that, if the observations lead to an effective averaging of the expansion rate over various directions similar to eq. (2.14), deceleration should be expected. If, however, the averaging is modified the expansion could be perceived as accelerating. This would happen in the case of an overdensity if the observations are more sensitive to the expansion along the radial direction. This is the case for an observer located in the center of an overdensity, who receives light signals only in the radial direction. Some of these signals originate in the regions outside the overdensity in which the local acceleration parameter is positive. The form of the luminosity distance as a function of the redshift in such a scenario provides another measure of the cosmological acceleration through eq. (5.14). The results depicted in figs. 7, 8 demonstrate the possible link between the growth of perturbations and the perceived acceleration of the expansion.

There are several points in our scenario that require further work. The location of the observer is constrained by the isotropy of the cosmic microwave background. Exact isotropy would require the observer to be located in the center of a spherically symmetric perturbation. Small deviations from complete isotropy, such as the difference of power between the northern and southern hemisphere or possible alignments of the low multipoles [20], could possibly allow for an off-center location as well. An alternative possibility is that the isotropy appears at a sufficiently large length scale in a configuration with several centers of symmetry. It is an interesting question whether the radial acceleration can be the dominant contribution for a random location of the observer.

The form of the expansion within a collapsing overdensity is another point that has to be addressed in future work. In our model the cosmological fluid within the overdensity is approximated as pressureless. As a result, the expansion for small redshifts is strongly decelerating. This makes the comparison with the supernova data problematic. A more sophisticated model is required in order to describe with quantitative accuracy both the cosmological expansion and the collapse of an overdense region.

Another issue concerns the existence of a characteristic scale for the inhomogeneity. In our simple model, it is apparent from figs. 7, 8 that the presence of acceleration at redshifts $z \sim 0.5$ forces the redshift of the surface of the overdensity to values $z_0 \sim 0.05$. On the other hand, it is remarkable that perturbations at the level of 10% in the present average density are capable of inducing acceleration in certain directions (see fig. 3). It is possible for such perturbations to be very extensive (of the order of 100 Mpc or even larger) without being in conflict with observations.

As a final remark we mention that a series of studies [21] has considered the possibility

that we are located within an underdense region of the Universe, while we receive light signals that originate outside this region. The luminosity-redshift relation in this case could be similar to the one in an accelerating homogeneous Universe. We have verified this conclusion within our model. The expansion is decelerating for all redshifts, but a significant reduction in the value of the Hubble parameter beyond a certain critical value $z_{cr} \sim 0.1$ can provide consistency with the supernova data.

Acknowledgments

We would like to thank M. Plionis for useful discussions. This work was supported by the research program “Pythagoras II” (grant 70-03-7992) of the Greek Ministry of National Education, partially funded by the European Union.

- [1] A. G. Riess *et al.* [Supernova Search Team Collaboration], *Astron. J.* **116** (1998) 1009 [arXiv:astro-ph/9805201]; *Astrophys. J.* **607** (2004) 665 [arXiv:astro-ph/0402512]; S. Perlmutter *et al.* [Supernova Cosmology Project Collaboration], *Astrophys. J.* **517** (1999) 565 [arXiv:astro-ph/9812133].
- [2] W. J. Percival *et al.* [The 2dFGRS Collaboration], *Mon. Not. Roy. Astron. Soc.* **327** (2001) 1297 [arXiv:astro-ph/0105252]; J. L. Sievers *et al.*, *Astrophys. J.* **591** (2003) 599 [arXiv:astro-ph/0205387].
- [3] D. N. Spergel *et al.* [WMAP Collaboration], *Astrophys. J. Suppl.* **148** (2003) 175 [arXiv:astro-ph/0302209].
- [4] E. W. Kolb, S. Matarrese, A. Notari and A. Riotto, arXiv:hep-th/0503117; P. Martineau and R. Brandenberger, arXiv:astro-ph/0510523.
- [5] C. M. Hirata and U. Seljak, *Phys. Rev. D* **72** (2005) 083501 [arXiv:astro-ph/0503582]; C. Wetterich, *Phys. Rev. D* **67** (2003) 043513 [arXiv:astro-ph/0111166]; G. Geshnizjani, D. J. H. Chung and N. Afshordi, *Phys. Rev. D* **72** (2005) 023517 [arXiv:astro-ph/0503553]; E. E. Flanagan, *Phys. Rev. D* **71** (2005) 103521 [arXiv:hep-th/0503202].
- [6] R. C. Tolman, *Proc. Nat. Acad. Sci.* **20** (1934) 169; H. Bondi, *Mon. Not. Roy. Astron. Soc.* **107** (1947) 410.
- [7] S. Rasanen, *JCAP* **0411** (2004) 010 [arXiv:gr-qc/0408097]; arXiv:astro-ph/0504005.
- [8] J. W. Moffat, *JCAP* **0510** (2005) 012 [arXiv:astro-ph/0502110]; arXiv:astro-ph/0505326.
- [9] H. Alnes, M. Amarzguioui and O. Gron, arXiv:astro-ph/0506449.
- [10] N. Mustapha, C. Hellaby and G. F. R. Ellis, *Mon. Not. Roy. Astron. Soc.* **292** (1997) 817 [arXiv:gr-qc/9808079].
- [11] M. N. Celerier, *Astron. Astrophys.* **353** (2000) 63 [arXiv:astro-ph/9907206];
- [12] H. Iguchi, T. Nakamura and K. i. Nakao, *Prog. Theor. Phys.* **108** (2002) 809 [arXiv:astro-ph/0112419]; Y. Nambu and M. Tanimoto, arXiv:gr-qc/0507057.
K. Bolejko, arXiv:astro-ph/0512103;
R. Mansouri, arXiv:astro-ph/0512605;
R. A. Vanderveld, E. E. Flanagan and I. Wasserman, arXiv:astro-ph/0602476.
- [13] R. R. Caldwell, *Phys. Lett. B* **545** (2002) 23 [arXiv:astro-ph/9908168];

S. M. Carroll, M. Hoffman and M. Trodden, Phys. Rev. D **68** (2003) 023509 [arXiv:astro-ph/0301273].

[14] P. S. Joshi and I. H. Dwivedi, Phys. Rev. D **47** (1993) 5357 [arXiv:gr-qc/9303037].

[15] H. Bondi, Rev. Mod. Phys. **29** (1957) 423.

[16] G. W. Gibbons, S. A. Hartnoll and A. Ishibashi, Prog. Theor. Phys. **113** (2005) 963 [arXiv:hep-th/0409307].

[17] J. E. Gunn and J. R. I. Gott, Astrophys. J. **176**, 1 (1972);
 A. Cooray and R. Sheth, Phys. Rept. **372** (2002) 1 [arXiv:astro-ph/0206508].

[18] D. F. Mota and C. van de Bruck, Astron. Astrophys. **421** (2004) 71 [arXiv:astro-ph/0401504].

[19] M. H. Partovi and B. Mashhoon, Astrophys. J. **276** (1984) 4;
 N. P. Humphreys, R. Maartens and D. R. Matravers, Astrophys. J. **477** (1997) 47 [arXiv:astro-ph/9602033].

[20] A. de Oliveira-Costa, M. Tegmark, M. Zaldarriaga and A. Hamilton, Phys. Rev. D **69** (2004) 063516 [arXiv:astro-ph/0307282];
 H. K. Eriksen, F. K. Hansen, A. J. Banday, K. M. Gorski and P. B. Lilje, Astrophys. J. **605** (2004) 14 [Erratum-ibid. **609** (2004) 1198] [arXiv:astro-ph/0307507];
 D. J. Schwarz, G. D. Starkman, D. Huterer and C. J. Copi, Phys. Rev. Lett. **93** (2004) 221301 [arXiv:astro-ph/0403353].

[21] K. Tomita, Astrophys. J. **529**, 26 (2000); Astrophys. J. **529**, 38 (2000); Mon. Not. Roy. Astron. Soc. **326** (2001) 287 [arXiv:astro-ph/0011484].